Analog multiplexer for testing multianode photomultipliers used in AMIGA project of the Pierre Auger Observatory

2015 JINST 10 T09004

(http://iopscience.iop.org/1748-0221/10/09/T09004)

PUBLISHED BY IOP PUBLISHING FOR SISSA MEDIALAB

RECEIVED: *July 2, 2015*
ACCEPTED: *August 19, 2015*
PUBLISHED: *September 17, 2015*

TECHNICAL REPORT

Analog multiplexer for testing multianode photomultipliers used in AMIGA project of the Pierre Auger Observatory

A. Lucero,[a,c,1] **A. Almela,**[a,c] **F. Suarez,**[a,c] **C. Reyes,**[a] **A. Cancio,**[b] **A. Fuster,**[a,c] **F. Gallo,**[a,c] **M.R. Hampel,**[a,c] **M. Platino,**[a] **M. Videla,**[a] **O. Wainberg,**[a,c] **D. Yelos,**[b] **and A. Etchegoyen**[a,c]

[1] *Instituto de Tecnologías en Detección y Astropartículas (CNEA, CONICET, UNSAM), Centro Atómico Constituyentes, General Paz 1499, (B1650KNA) San Martín, Buenos Aires, Argentina*

[1] *Instituto de Tecnología en Detección y Astropartículas (CNEA, CONICET, UNSAM), Regional Mendoza, Comisión Nacional de Energía Atómica, Figueroa Alcorta 122, (5501) Godoy Cruz, Mendoza, Argentina*

[1] *Universidad Tecnológica Nacional, Facultad Regional Buenos Aires, Medrano 951, (C1179AAQ) Buenos Aires, Argentina*

E-mail: agustin.lucero@iteda.cnea.gov.ar

ABSTRACT: Most particle detectors used in astroparticle physics have an optoelectronic device that senses generated light and converts it into an electrical pulse. Photomultiplier tubes are commonly used, particularly those with multiple anodes. Prior to coupling to a detector system these tubes must be fully characterized, which requires either the same number of data acquisition channels as outputs or a switching-multiplexer system. Given that every project has its own requirements, the testing system must be as flexible as possible. The multiplexer presented here can be used to test silicon photomultipliers or any high-frequency signal. It is a scalable 64 to 4 channel analog device designed for low crosstalk and low attenuation. Results of the application of this multiplexer with a -3 dB bandwidth of 800 MHz are shown by testing 64-channel tubes for the AMIGA project.

KEYWORDS: Photon detectors for UV, visible and IR photons (vacuum) (photomultipliers, HPDs, others); Data acquisition concepts; Particle detectors

[1] Corresponding author.

doi:10.1088/1748-0221/10/09/T09004

2015 JINST 10 T09004

Contents

2015 JINST 10 T09004

1 Introduction

The Pierre Auger Observatory [1] studies the most energetic subatomic particles known in nature, ultra high-energy cosmic rays. They arrive from outer space to the upper layers of the atmosphere and produce particle air showers that reach the surface of the Earth. The Auger Observatory was designed to detect cosmic rays with energies above 10^{18} eV. Air showers induced by cosmic rays have two main components: electromagnetic (electrons and photons) and muonic. The Auger Observatory consists of 27 fluorescence telescopes, which detect the light produced by the air-shower electrons as they traverse the atmosphere and $\sim$ 1660 surface detectors, which measure both the electromagnetic and muonic air-shower components at the ground. The AMIGA ("Auger Muon and Infill Ground Array" project is designed to directly measure the muonic component [2]. The main aims of this enhancement are to better discriminate between primary particles of different chemical composition and to detect particle showers with a lower energy threshold than the original Auger Observatory design. Each AMIGA station consists of an arrangement of a standard Auger surface detector (see figure 1 left) and three 10 m^2 rectangular muon detector modules, which sum to a total detection area of 30 m^2. The muon detector module is comprised of 64 scintillator bars [3] with a wavelength shifter (WLS) optical fiber along each bar. These optical fibers collect light generated in the scintillating material by charged particles and propagate the photons toward a 64 pixel Hamamatsu multianode photomultiplier tube (MaPMT) H8804-200MOD. The photo-electrons generated in a MaPMT pixel produce an amplified signal that undergoes discrimination

by a comparator in the front-end electronics of the AMIGA detectors. The generated digital pulse is sampled and acquired by an FPGA at 320 MHz (3.125 ns sampling rate) generating a "0" or "1" bit that represents the respective absence or presence of a signal [4].

Because MaPMTs are fundamental components of the acquisition electronics, each must be fully characterized prior to deployment at the Observatory site. The most relevant parameters to muon counting are the single photo-electron (SPE) spectrum, inter-channel cross talk (XT) and dark-pulse rate (DR) [5]. Once completed, AMIGA will have 61 stations, which corresponds to a total of 183 MaPMTs (excluding spares). All these PMTs must be characterized with a test system capable of processing the 64 outgoing signals as individual PMTs.

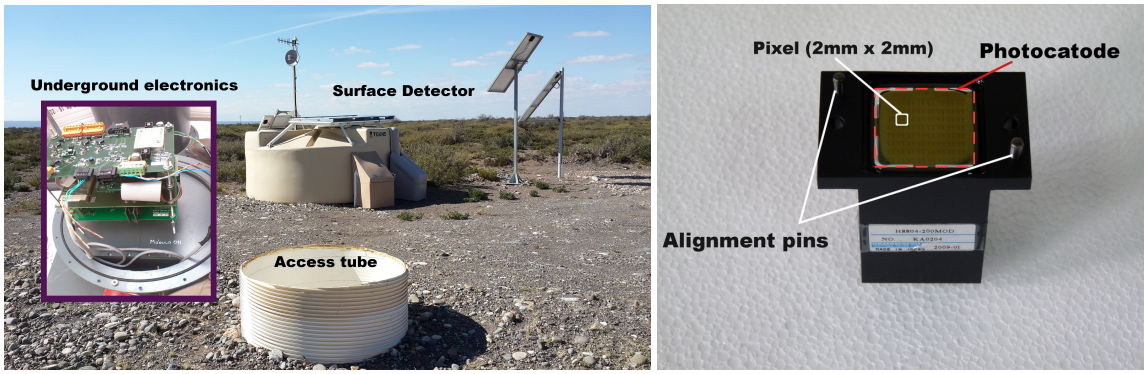

Figure 1. Left: Auger Observatory surface detector, muon detector access tube and underground electronics. Right: MaPMT H8804-200MOD from Hamamatsu.

2 AMIGA PMT testing requirements

An H8804-200MOD MaPMT manufactured by Hamamatsu is shown in figure 1 (right). Its main features are the ultra Bi-alkali (UBA) photo-cathode and the 8×8 array of square anodes, each one with its own 12-stage metal-dynode multiplication chain (R-7600-M64) [6]. Depending on the photo-cathode region (also called a "pixel") on which the impinging photons land, the SPEs are guided by the focussing electrodes towards a given dynode channel in which they are multiplied and finally collected by their respective anodes. In this way, an MaPMT behaves as a matrix of 64 individual PMTs with the same high voltage (HV) configuration. The high quantum efficiency and the large number of pixels are features that make this PMT an excellent device for the AMIGA detector design.

PMTs and each of their pixels are tested on a test bench designed for complete and automated evaluation. The schematic diagram is displayed in figure 2. The setup consists of a pulsed light source (LS) composed of 64 blue LEDs (each one with an individually controlled intensity) plus their respective drivers. These LED sources are used to generate light pulses with intensities similar to those produced by one particle passing through a scintillator bar at different distances from the MaPMT. Each LED is able to generate light intensity from SPE level to ~ 30 photo-electrons.[1]

The 64 LEDs are coupled to the MaPMT pixels via WLS fibers (green arrow in figure 2), which in turn are glued to a coupling device similar to those used in the AMIGA detector modules.

[1] The LED-driver generates a current pulse of variable amplitude and FWHM$\simeq$ 6 ns.

2015 JINST 10 T09004

Then, a four-layer custom designed board (socket board) with 64 low-noise and low-attenuation coaxial cables (RG178 BELDEN RF100LL 7805R) is used to carry the signals to the switching system: the analog multiplexer (Mux). This multiplexer is responsible for switching the different 64 PMT output signals onto the 4 inputs signals of the data acquisition system (DAQ, LeCroy oscilloscope). The power-supply and monitoring block supplies HV to the MaPMT and monitors the system variables (temperature, HV, LS supply). Finally, the system control and signal processing are performed with a server running a C++ program for an on-line and automated data analysis including plot generation.

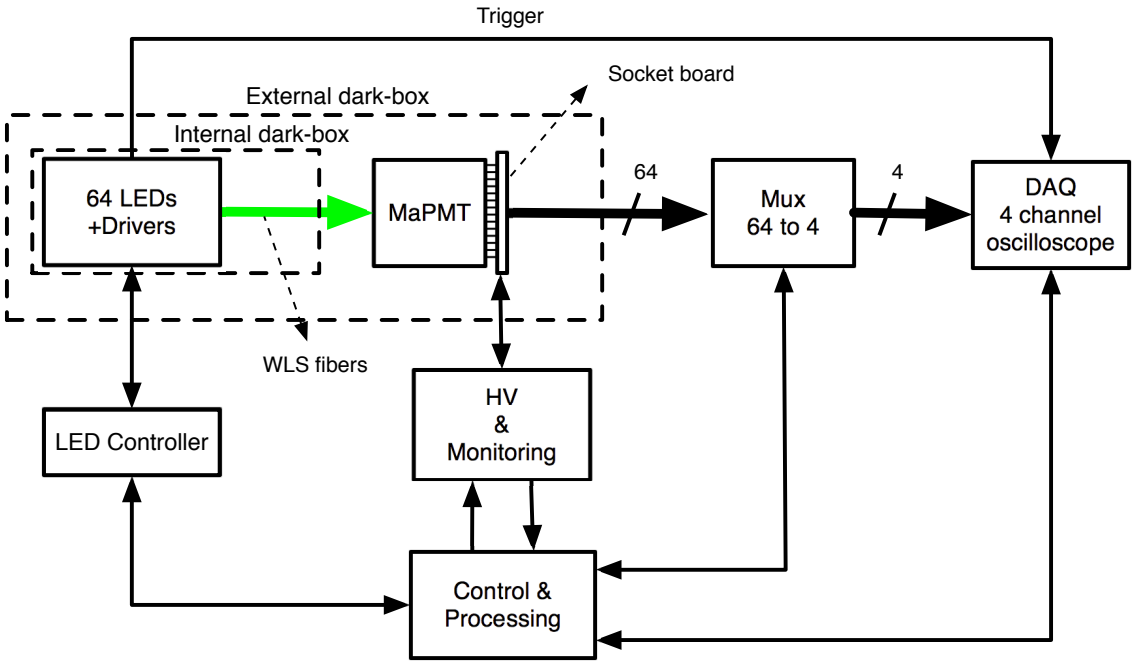

Figure 2. Setup of the test-bench used to characterize the AMIGA H8804-200MOD MaPMTs

Light pulses generated by the LS are transported by WLS optical fibers onto each MaMPT pixel. The light intensity depends on the test performed e.g. SPE or XT. The MaPMT transforms light into short (~ 1.3 ns SPE FWHM) current pulses, which are guided by the Mux to the DAQ system that provide the proper $50\,\Omega$ termination for the MaPMT output. Once digitized and stored, the signals are processed and the resulting data analyzed to fully characterize the MaPMT. As already mentioned, each step in the testing method, as well as the LS intensity, are continuously adjusted by the control block.

The science objectives of the AMIGA project drove the detector design, which in turn drove the PMT requirements and characteristics to be tested. These are:

- **SPE peak distribution** (SPE_{peak}): it is essential to measure peak-amplitude distributions since the 1-bit digitization is performed by adjustable-threshold discriminators. The discrimination level would be set based on the pixel mean SPE amplitude.
- **SPE charge distribution** (SPE_Q): each pixel gain is measured by determining a SPE charge spectrum. The gain uniformity is observed in the distribution of the 64-pixel gains. This test

2015 JINST 10 T09004

permits one to normalize each pixel anode charge in an XT evaluation [7]. Gain uniformity may be used for air shower simulations and to calibrate the AMIGA scanner system (i.e. by conversion of collected charge to number of SPEs), which is part of the quality assurance plan of the module fabrication process [8].

- **SPE pulse width resolution** (t_{FWHM}): although the trigger level is set on the SPE amplitude, the SPE identification is performed by the FPGA based on the time elapsed over which the signal remains above the discrimination level.
- **Dark Pulse Rate** (DR): the MaPMT dark-rate (sum of 64 channels) is the total number of anode pulses per second above a certain threshold, when the photo-cathode is isolated from all external light sources. This is another important parameter since DR pulses may lead to muon over-counting.
- **Cross talk** (XT): it is the ratio of the number of SPEs between two anodes when only one of them is excited. This is the largest source of systematic counting uncertainty that might lead to muon over-counting. It is also the most challenging parameter to measure since the output of each pixel must be compared with each of its neighbouring pixels (up to 8) and the switching of PMT output signals is very complex when using a 4 channels acquisition system. All tests need a Mux, particularly the XT test.

Instead of charge-to-digital converters (as done in the Auger Observatory PMT test facility [9]), this test system uses voltage digitizers (ADC: analog-to-digital converter). ADCs allow one to measure signal amplitudes and time resolution down to the SPE level. The DAQ system is a four channel Wavepro 7Zi-A LeCroy oscilloscope with 1.5 GHz bandwidth and 10 GS/s maximum sampling rate per channel [10]. Optimal work conditions for the test system (considering parameter resolution and processing time) are reached by operating the oscilloscope at a sampling rate of 5 Gs/s (200 ps sampling interval), 1000 samples per waveform and a vertical scale of 20 mV/div with 50 Ω termination.

3 Multiplexer design and construction

The automatic Mux is an electronic device specifically designed to avoid changing cabling manually. It performs the switching of input signals, which allows one to test a complete PMT in a reasonable period of time. A high-frequency multiplexer was built to meet the design requirements described below:

3.1 Design requirements

- Optimal insertion-loss and bandwidth features to ensure signal integrity.
- Low capacitive XT between neighbouring channels in order to avoid introduction of systematic uncertainties during XT measurements. This is a challenge when working with high bandwidth signals.
- Data acquisition for each MaPMT pixel must be performed with at least 3 neighbouring channels simultaneously.

2015 JINST 10 T09004

- A 50 Ω resistor must be present for each MaPMT pixel not connected to any oscilloscope channel. This avoids changing channel load conditions when set to testing.
- Constancy of the characteristic impedance (50 Ω) along the transmission line. This is to avoid reflections that produce signal distortion and increase the return loss.
- All transmission lines should introduce the same delay as well as the same insertion loss (uniformity).
- Fast and easy maintenance to avoid MaPMT testing delays during the several years of AMIGA construction and operation ($\sim$ 15 years).
- Scalable number of input and output channels to allow re-configuration of the test facility for different devices.

To meet the requirements described above, a modular design was proposed as shown in the diagram of figure 3. It simplifies the Mux construction and maintenance.

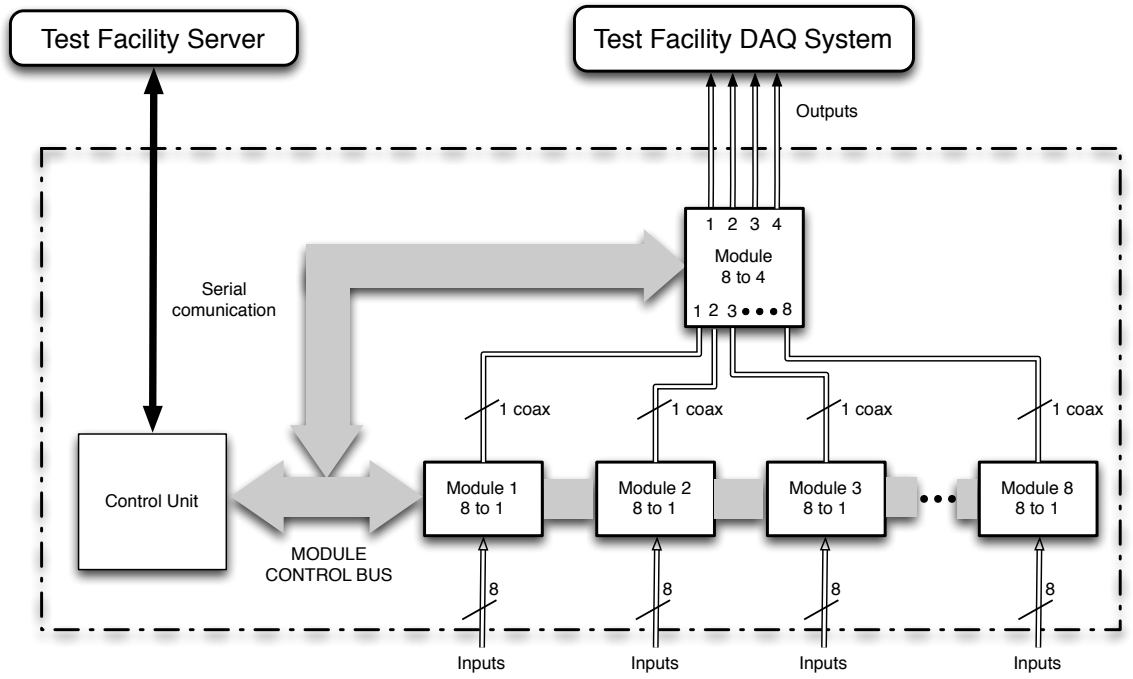

Figure 3. The 64:4 multiplexer modular scheme.

The whole Mux structure consists of eight 8:1 switching modules (slave modules), which are connected with coaxial cables to a single 8:4 module (master module). This master module comprises four 2:1 multiplexers and one to two slave modules are assigned to each. Thus, the overall topology may also be seen as a regular four 16:1 multiplexer. The requirements imposed by the XT test (each pixel may be measured simultaneously with every neighbour) are accomplished by a correct matching between PMT outputs and Mux inputs (figure 4). This connection scheme has the additional advantage of connecting neighbouring pixels to different slave modules to prevent

2015 JINST 10 T09004

electromagnetic coupling between channels which may lead to XT noise. Finally, all of the analog modules (master and slaves) are connected to a control bus together with a digital controller unit used as interface to the main computer of the PMT test facility.

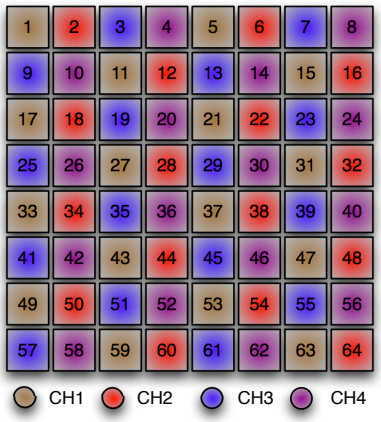

Figure 4. Connection setup between MaPMT outputs (numbers) to multiplexer outputs (oscilloscope ch.). The 8×8 matrix corresponds to the PMT pixel configuration. Any pixel may be acquired simultaneously with each adjacent pixel.

3.2 Analog boards: design, simulations, and implementation

The analog boards are the most important parts of the Mux. Their aim is to transmit the signals from the PMT anodes to the DAQ without detriment to the signal quality (i.e. attenuation, bandwidth, signal to noise ratio) which may introduce additional uncertainties in the measured parameters. As such, special care was taken both when designing the transmission lines and when selecting the switching device.

The SPE signal for the AMIGA PMTs is a very narrow signal with a wide bandwidth and a very low amplitude despite a working amplification of around $\times 10^6$. As such, the SPE signal defines the bandwidth needed for the Mux system. It can be approximated by a gaussian function which frequency spectrum, also a gaussian, has a cut-off frequency that defines its -3 dB bandwidth.[2] The 3 dB bandwidth relates to the pulse width (t_{FWHM} in seconds) as shown in eq. (3.1) [11]:

$$BW_{3\mathrm{dB}} = \frac{0.35}{t_{\mathrm{FWHM}}} \tag{3.1}$$

Thus, the required bandwidth is nearly 300 MHz for an average gaussian SPE pulse width of about 1.3 ns (figure 5). Therefore, at least twice this calculated bandwidth was aimed for in the design, i.e. a bandwidth ≥ 600 MHz (or more) for each channel of the multiplexer (PCB plus relays and connectors), to avoid having the -3 dB attenuation at the highest frequency of the pulse.

The HF3 Axicom series, specifically the HF3-52 model, was chosen as the main switching device because of its excellent transmission characteristics and small size. This device is a Single Pole Double Throw (SPDT) relay which was specially designed to operate with frequencies up to 3 GHz (with a 50 Ω characteristic impedance over the whole frequency range) [12]. The low

[2]Frequency bandwidth in which the spectrum energy density is greater than or equal to 50% of its maximum value.

2015 JINST 10 T09004

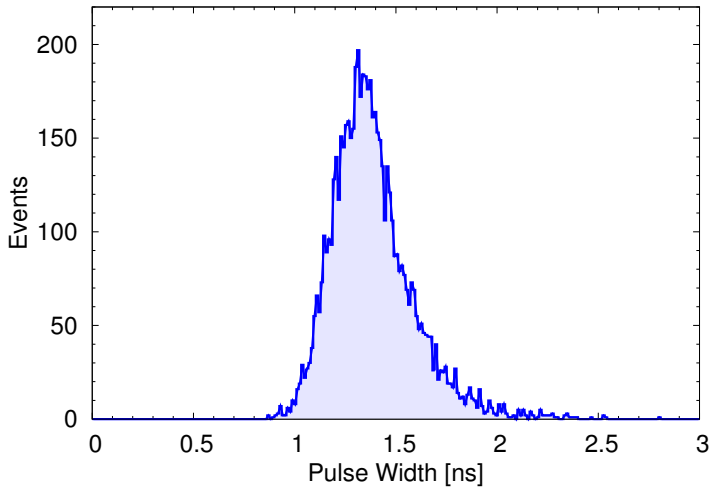

Figure 5. FWHM histogram of SPE pulse widths from a pixel of a H8804−200MOD PMT with a 50 Ω load. Measurement were performed at PMT test facility at ITeDA (without the Mux).

insertion loss, excellent linearity, high insulation and especially the thermal independence of these RF features, make it superior to other relays such as both solid-state (GaAs FET, Pin Diode) and RF-MEMs relays [13]. Disadvantages compared to other relays, particularly to that of solid state relays, are its size (prevents large scale integration) and low switching speed. However, these drawbacks are not significant for the Mux construction and operation.

The transmission lines were coplanar wave-guides (CPWs) because they present a good compromise between insertion loss, return loss, and insulation regarding other wave-guide types (e.g. the microstrip and stripline) [14]. In particular, high insulation decreases XT due to electromagnetic coupling between neighbouring lines within the same analog module.

The boards used to perform the transmission lines are the double layer substrate RO4356 [15] from Rogers with 0.762 mm thickness (30 mils) and a dielectric constant $\epsilon_r = 3.66$. These boards show high thermal stability, characteristic impedance stability, and very low insertion loss ($\simeq$ 0.1 dB/inch at 3 GHz) in comparison to the regular FR-4 (flame retardant 4) boards. All of the recommendations from the relay manufacturer [16] were complied with. Additional special care was taken in the design and simulations of bends and junctions to improve the EMC (Electromagnetic Compatibility) of channels and modules.

The slave module topology was implemented with a total of 11 relays arranged in three levels. The first level consists of 8 relays which form quad 2:1 50 Ω terminated multiplexers (a 50 Ω termination is chosen for input channels disconnected from the Mux output). As seen in figure 6 (left), the common output of each terminated multiplexer is the physical attachment of two relay outputs made by a CPW. It forms a "Y" junction that adds a negligible capacitive load and an RF stub to the transmission line (minimized by an optimal design). It was decided to use the junction instead of inserting an additional relay because each additional relay adds a further attenuation step and increases the density of the control lines. The second level consists of two more relays that link the outputs of the two consecutive relays from the first level. Finally, the third level consists of a single relay which connects the level 2 relay outputs to the slave module output (figure 6 right).

2015 JINST 10 T09004

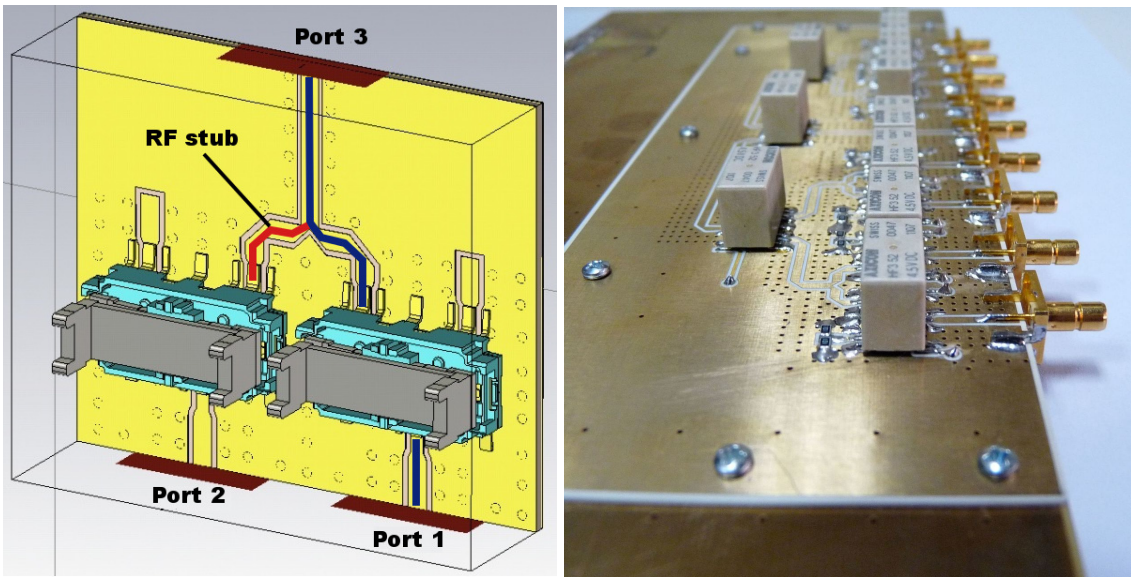

Figure 6. Left: Model of the 2:1 terminated multiplexer used for simulation. Right: Final version of the analog board of a slave module.

The master module is a quad 2:1 non-terminated Mux implemented with a single HF3-52 relay (figure 7). As for the slave modules, each wave guide is located at a safe distance and surrounded by via holes (via fences) to improve EMC and reduce cross talk between CPWs [17]. All of the analog transmission lines are located on the upper layer of the RO4356 board. The bottom layer is used for the ground plane and to insulate the analog lines from the control ones. The control lines were implemented on an extra PCB on a FR-4 board located below the analog board. This also gives mechanical support for the latter (see figure 7). Finally, golden SMB connectors were chosen for both input and output channels due to their high performance and ease to plug/unplug.

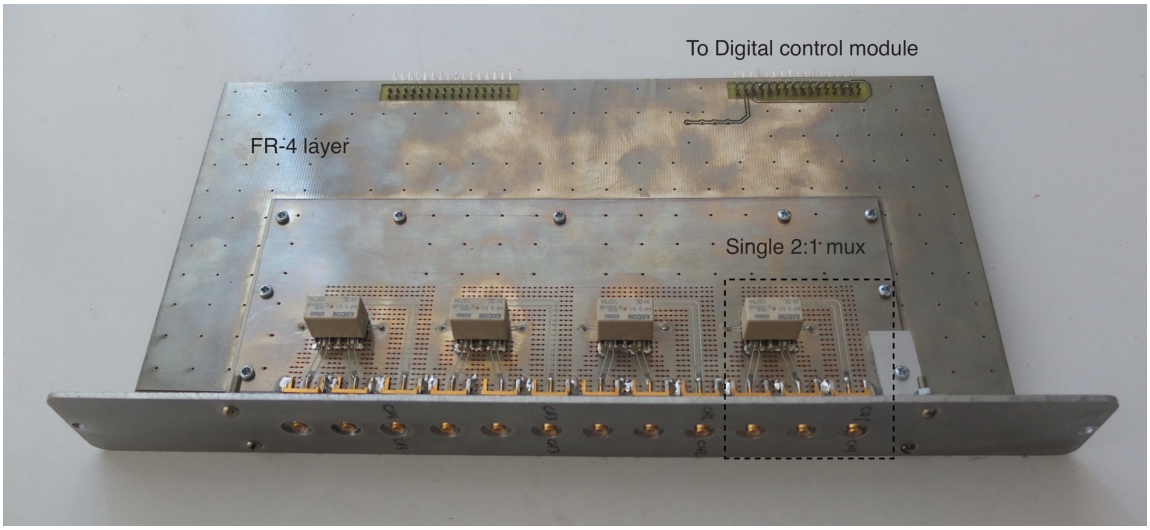

Figure 7. Master 8:4 module made by four isolated 2:1 multiplexers.

2015 JINST 10 T09004

Analog board optimization was performed by simulating the electromagnetic component (up to 3 GHz) using the Finite Element Analysis (FEA) HFSS software package provided by Ansoft. The goal of the simulations was to verify the transmission characteristics of the CPWs, their coupling with the HF3-52 relay, and the insulation between them, prior to this module's construction. Simulations were also useful in the design and adjustment of the RF stub, which was the most critical issue in the slave-module design. Prototypes of the 2:1 multiplexers (figures 6 left and 8 left) were built to confirm i) the simulation results (figure 8 right) and ii) the input reflection (S_{11}) and forward transmission coefficients (S_{31}). Data[3] and simulations matched as expected thus fully confirming the scheme proposed for this critical section of the analog boards.

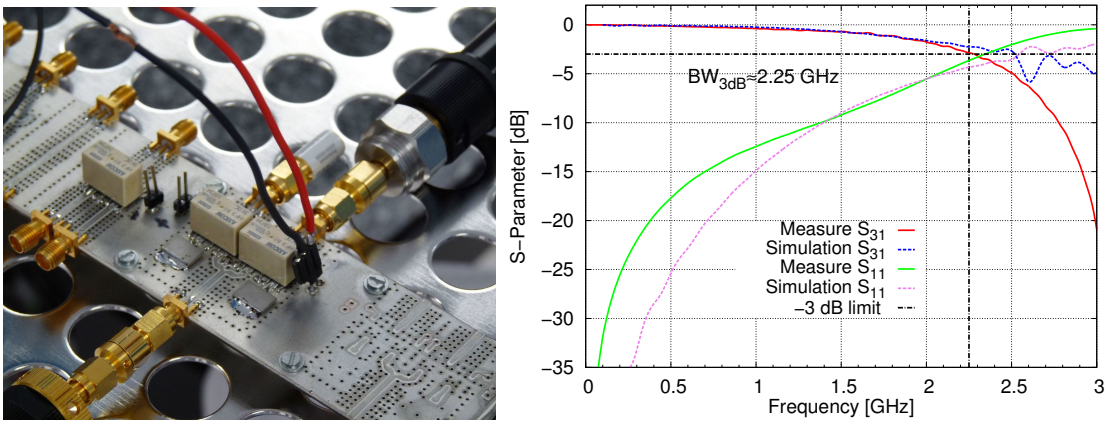

Figure 8. Left: First 2:1 Mux prototype manufactured at ITeDA. Right: data and simulation results. (S_{11}) and (S_{31}) are the respective input reflection and forward transmission coefficients.

3.3 Digital boards: design and implementation

The digital control comprises a Control Unit (CU) and the digital control electronics of the analog modules (module's digital boards), which are connected through a digital parallel bus (figure 3). The CU is the interface between the test-facility computer and the modules. The digital boards of the modules are positioned together with each analog board and control the switching of the relays. The parallel bus is controlled by the CU and can be expanded to connect more modules in order to increase the multiplexer channels, which allow to test more than one MaPMTs at the same time (or a photo-detector with more than 64 channels). Special care was taken when designing the digital board of the modules to avoid introducing digital interference in the analog wave-guides.

3.3.1 Control unit and data bus

The CU was implemented with a micro-controller (μC) Silicon Labs C8051F351 [18] which was programmed to communicate via a serial RS-232 port to the system main computer. The computer sends commands to the CU. They are coded into low-level instructions as digital signals in the μC ports. Each micro-controller has dual 8-bit parallel ports. Four bits of port 1 identify the chosen module (ID) while the remaining bits send the instructions (data). Port 2 is used for bus control signals (CLK, R/W, ALE, DataReady, ACKBUS) and RS232 serial communication.

[3] A Vectorial Network Analizer Agilent E8363B was used for these measurements.

2015 JINST 10 T09004

The μC was programmed to respond to the serial port with an interactive prompt terminal. It can be controlled with commands manually sent from any computer terminal. Nevertheless, C++ libraries were also written to allow Mux operation in a fully programmable and automated mode.

The digital bus between CU and digital boards was implemented on a bus board that supports the digital lines (control, data, and address lines) and also powers supply lines to both modules and CU.

3.3.2 Module's digital board

The digital board (figure 9) is split into two digital stages. The first one has a programmable logic to communicate with the parallel bus. The second stage has a discrete logic which decodes the CU commands and controls the analog-board relays. Stage one was built with a complex programmable logic device (CPLD) ALTERA MAXII EPM1270T144C5N [19] in which a basic communication protocol and several ports were implemented. These ports are required to communicate with i) the CU (data, address, and control), ii) the ID port used to configure the module address, and iii) an instruction port that sends the data word to the discrete logical stage. When the CU receives the command, it generates the address and the data word. It then sends the address and waits for a module acknowledgement (ACK). All modules receive the address word but only one module is identified by comparing its ID word with the address. The identified module sends the ACK signal, receives the data word and forwards it to the discrete stage through the instruction port.

The discrete stage is a decoder that uses a 6 bit word coming from the CPLD (through the opto-couplers) to control the module relays. Only 6 bits are used to avoid adding a large number of opto-couplers. Four bits are used to generate the nine different states of the modules while the remaining two are used to enable the decoder and for synchronization purposes. Note that this decoder is not needed to control the master module since it only has 4 relays, so the outputs from the opto-couplers are routed directly to a 6 bit port.

The discrete logic stage directly controls each relay, so EMC considerations were taken into account to avoid introducing digital noise into the analog wave-guides. These considerations involve the use of a combinational logic circuit, which does not require clock signals, and opto-couplers to avoid digital noise coming from the CPLD. Additionally, the discrete logic power supply and its ground reference are also isolated from the bus by using a DC-DC converter.

3.4 Mechanical assembly

The Mux was built in a crate that holds the bus board, nine modules (eight slave modules and one master module), the CU, and the power supply. The crate can accommodate more modules if needed. It is mounted on a rack to ease connections with the rest of the test-facility devices (figure 10).

4 Performance verification tests

Performance verification was accomplished by comparing data taken with and without the multiplexer; SPE signals and XT parameters were measured 50 times for a H8804-200MOD MaPMT. It is important to note that $\sim 10,000$ SPE and ~ 600 XT pulses (in each neighbouring pixel) were required for each of the 50 runs. These two tests are the most critical because they set the PMT absolute gain and the inter-channel EMC.

2015 JINST 10 T09004

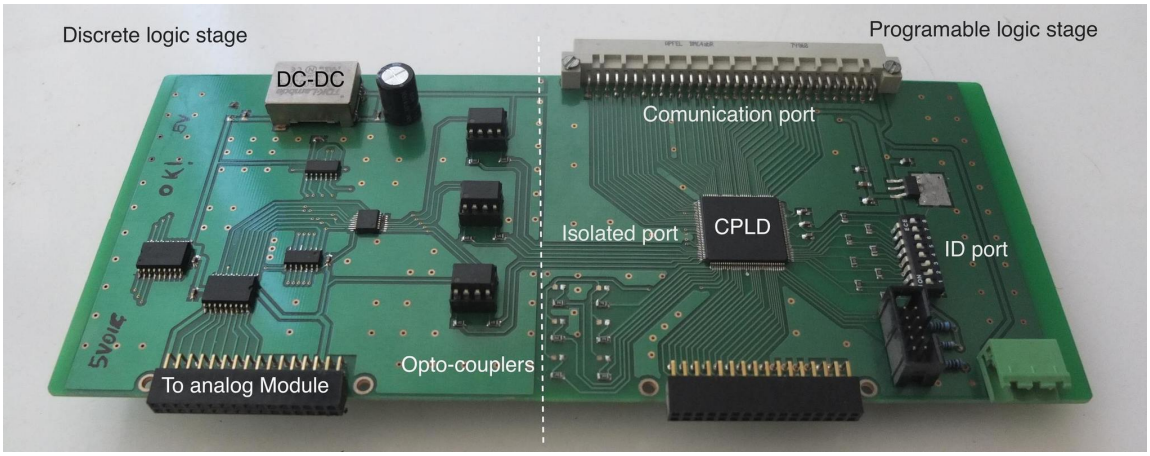

Figure 9. Digital board to control the relays of analog modules and to communicate with the CU.

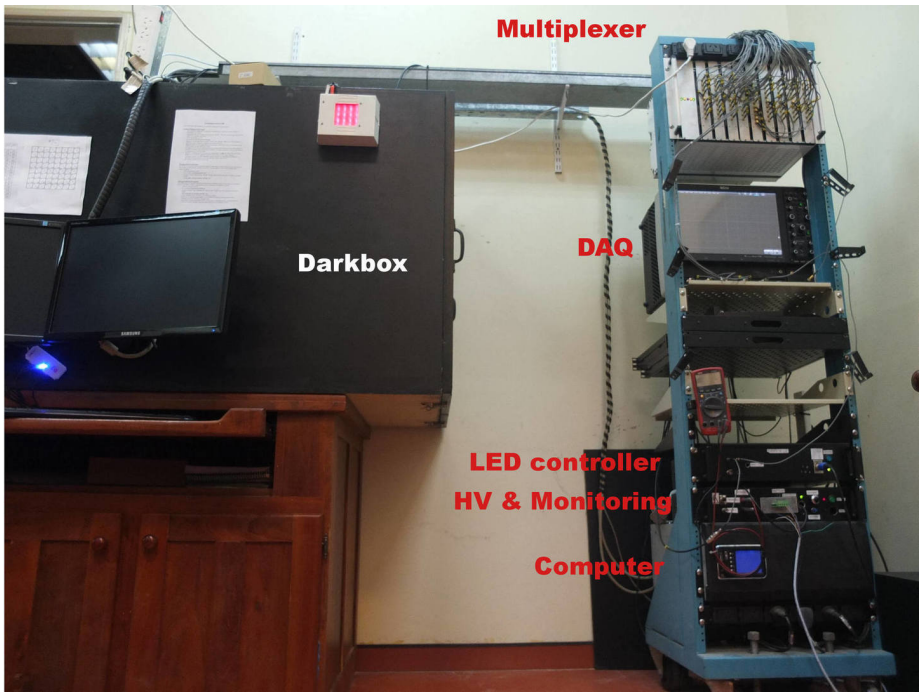

Figure 10. PMT test system. The Mux is located on top of the rack as close as possible (reduced cabling length) to the darkbox containing the PMT being tested. The CU is the white module on the left hand side of the Mux. The rest of the modules are the slave (four at each side) and the master (at the center) modules.

The complete set of measurements was performed on 4 pixels located in different areas of photo-cathode: pixel 8 (corner pixel), 18 (inner pixel), 41 (border pixel), and 47 (inner pixel), see figure 4. The SPE data comparisons with and without the multiplexer (figure 11 top left and 11 top right) show that there are negligible decreases in the SPE_{peak} and increases in the t_{FWHM}: there is only a slight attenuation of the higher frequency components of the signals. The relative errors (figure 11 bottom) are $\leq 5\%$ which bears no impact on the performance of the detector system. Also, a comparison of RMS_{baseline} values, used as a noise level estimator, does not present a noticeable

2015 JINST 10 T09004

increment, as expected after the careful EMC design.

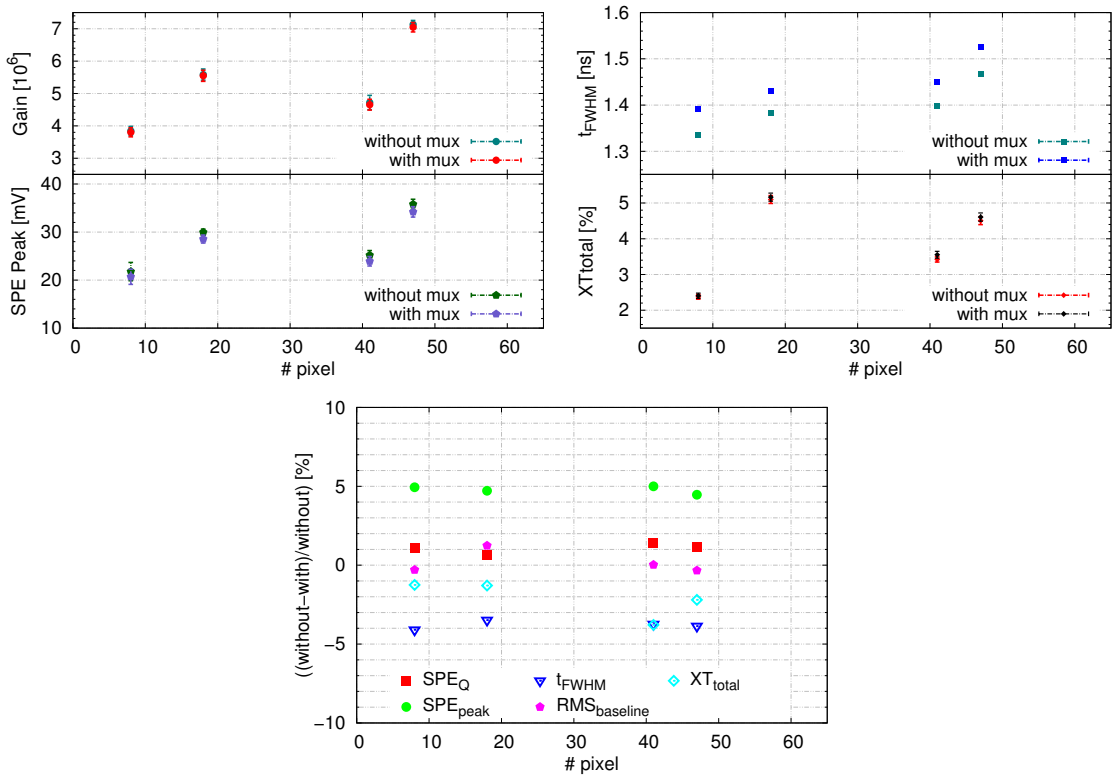

Figure 11. SPE signal measurements performed with and without the multiplexer. Dots are an average over 50 independent measurements with uncertainty bars representing the distributions' RMS values. The lower plot shows data relative uncertainties from the two upper panels; the discrepancy is always $\leq 5\%$.

These satisfying results confirm that the Mux does not introduce significant attenuation, noise, cross talk, signal rebound, or other undesired effect.

5 Results

The test system with the final Mux version (figure 10) was used to run a complete test over the 64 pixels of a H8804-200MOD Hamamatsu MaPMT. The -3 dB bandwidth from a Mux input to a Mux output was measured to be ~ 800 MHz (bandwidth of the slave and master module channel plus cabling and connectors). A complete MaPMT test comprises SPE measurements (including SPE_Q, SPE_{peak}, and t_{FWHM}), XT_{total}, and DR for each of the 64 pixels. This test was performed at three different HV levels: -900 V, -950 V, and -1000 V. Once the MaPMT is turned on and biased, the system requires ~ 5 hr. in order to cool down the photo-sensitive materials and to stabilize the pixel gains. During the testing period, which takes 15 hr. (~ 5 hr. for each voltage), the test system changes the cabling status automatically more than 600 times without human intervention.

Figure 12 (Top left) shows the gain and peak curves as a function of HV, where the values are the means over the 64 pixels. The maximum values in the total XT uniformity graph (figure 12 top right) correspond to the inner pixels while both corners and lateral pixels correspond to the

2015 JINST 10 T09004

minimum values since they have fewer neighbouring pixels. Unlike the XT, the DR uniformity presents a higher value for the lateral and corner pixels. As was studied in [20] this higher DR is believed to be due to an effect[4] that is a kind of cross-talk between any inner pixel and the pixels near the tube body. Finally, the pulse width histogram, t_{FWHM}, (figure 12 bottom) of all 64 pixels exhibits a high level of uniformity throughout the MaPMT.

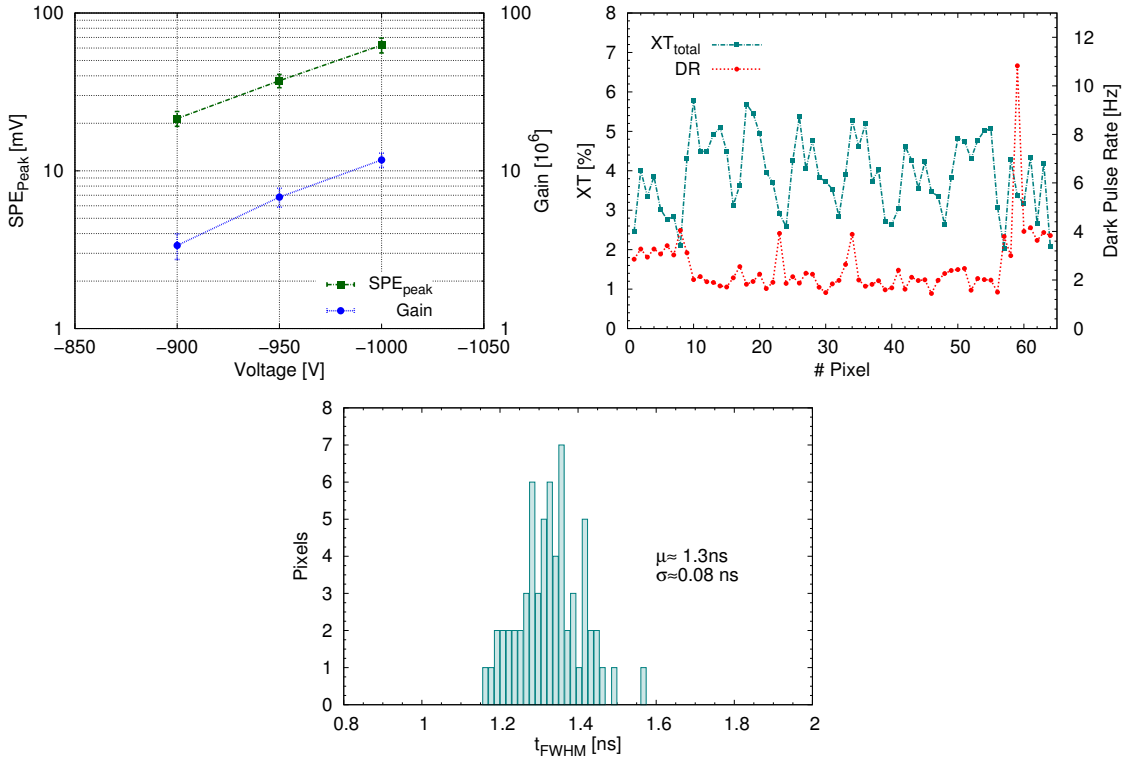

Figure 12. Test results of the 64 pixels of a H8804-200MOD Hamamatsu MaPMT using the multiplexer. Top left: Gain and SPE_{peak} vs. voltage averaged over the 64 pixels of the PMT. Top right XT_{total} and DR uniformity. Bottom: SPE signal pulse width (t_{FWHM}) histogram measured at -950 V.

6 Conclusions

A 64 to 4 analog multiplexer based on commercial HF relays was designed, built, and integrated in a test system. The switching sequence is fully programmable but may also be manually operated.

The performance of this multiplexer has been validated to be used for characterization of MaPMTs currently used in the AMIGA project. The Mux introduces an uncertainty in the SPE_{peak} and t_{FWHM} measurement of $\leq 5\%$. Gain, $\mathrm{XT}_{\mathrm{total}}$, and DR are not affected by use of the multiplexer. The absence of noise in the signals evidences the care taking in designing the multiplexer.

The PMT test facility is now fully automated and can provide all of the above-mentioned parameters for all PMT pixels in approximately 5 hr., for any given HV. This capability allows one

[4] Called "correlated pulses"

2015 JINST 10 T09004

to efficiently test all new PMTs during the production phase of the project and during maintenance and operation.

References

[1] PIERRE AUGER collaboration, A. Aab et al., *The Pierre Auger Cosmic Ray Observatory*, *Submitted to: Nucl. Instrum. Meth.* (2015) [arXiv:1502.01323].

[2] PIERRE AUGER collaboration, A. Etchegoyen, *AMIGA, Auger Muons and Infill for the Ground Array*, in *Proceedings of the 30th International Cosmic Ray Conference*, July 3-11, Mérida, México (2007) arXiv:0710.1646.

[3] PIERRE AUGER collaboration, A. Aab et al., *The Pierre Auger Observatory: Contributions to the 33rd International Cosmic Ray Conference (ICRC 2013)*, in *Proceeding of the 33rd International Cosmic Ray Conference*, July 2-9, Rio de Janeiro, Brazil (2013) arXiv:1307.5059.

[4] O. Wainberg et al., *Digital Electronics for the Pierre Auger Observatory AMIGA Muon Counters*, 2014 *JINST* **9** T04003 [arXiv:1312.7131].

[5] A.D. Supanitsky, A. Etchegoyen, G. Medina-Tanco, I. Allekotte, M.G. Berisso and M.C. Medina, *Underground Muon Counters as a Tool for Composition Analyses*, *Astropart. Phys.* **29** (2008) 461 [arXiv:0804.1068].

[6] Hamamatsu Phonotics K.K., *UBA, SBA Photomultiplier tube series*, http://www.hamamatsu.com/resources/pdf/etd/High_energy_PMT_TPMO0007E.pdf, 2008.

[7] F. Suarez, *Pierre Auger Observatory surface and underground detectors Operation and techniques*, dottorato di ricerca in fisica fondamentale, applicata ed astrofisica, Universià degli studi di Torino, 2008.

[8] M. Platino et al., *AMIGA at the Auger Observatory: The scintillator module testing system*, 2011 *JINST* **6** P06006.

[9] D. Barnhill, F. Suarez, K. Arisaka, B. Garcia, J.P. Gongora, A. Lucero et al., *Testing of photomultiplier tubes for use in the surface detector of the Pierre Auger Observatory*, *Nucl. Instrum. Meth.* **A 591** (2008) 453.

[10] Teledyne Lecroy, *WavePro 7 Zi/Zi-A Oscilloscopes — Getting Started Manual*, http://cdn.teledynelecroy.com/files/manuals/wp7zi-manual.pdf, (2013).

[11] S. Flyckt and C. Marmonier, *Photomultiplier tubes: principles and applications*, Phillips Photonics, Brive, 2002.

[12] Tyco Electronics Corporation, *Axicom HF3 RF signal Relay*, http://www.te.com/usa-en/product-1-1462051-6.html (2013).

[13] W. Johler, *RF performance of ultra-miniature high frequency relays*, in *Proceedings of the Forty-Ninth IEEE Holm Conference on Electrical Contacts* (2003) 179.

[14] T. Edwards and B. Steer, *Foundations of interconnect and microstrip design*, John Wiley and Sons, Inc., Chichester 2000.

[15] Roger corporation, *RO4000 Series High Frequency Circuit Materials*, http://www.rogerscorp.com/documents/726/acm/RO4000-Laminates—Data-sheet.pdf (2010).

[16] Tyco Electronics Corporation, *PCB design for axicom RF relays*, http://www.te.com (2009).

2015 JINST 10 T09004

[17] A. Suntives, A. Khajooeizadeh and R. Abhari, *Using via fences for crosstalk reduction in PCB circuits*, in proceedings of the *2006 IEEE International Symposium on Electromagnetic Compatibility (EMC 2006)* **1** (2006) 34.

[18] Silicon Laboratories, *C8051F351 Mixed-Signal MCU*, http://www.silabs.com/products/mcu/8-bit/c8051f51x/pages/c8051f51x.aspx (2005).

[19] Altera Corporation, *Max II Device Handbook*, http://www.altera.com/literature/hb/max2/max2_mii5v1.pdf (2009).

[20] K. Rielage et al., *Characterization of a multianode photomultiplier tube for use with scintillating fibers*, *Nucl. Instrum. Meth.* **A 463** (2001) 149.

2015 JINST 10 T09004